ELSEVIER

The Chemical Engineering Journal 59 (1995) 91–100

THE CHEMICAL ENGINEERING JOURNAL

# Effect of gas and liquid properties on gas phase dispersion in bubble columns

M.V. Kantak [a], R.P. Hesketh [a], B.G. Kelkar [b,*]

[a] *Department of Chemical Engineering, University of Tulsa, Tulsa, OK 74104, USA*

[b] *Department of Petroleum Engineering, University of Tulsa, Tulsa, OK 74104, USA*

Received 2 September 1993; accepted 14 September 1994

**Abstract**

The effect of gas and liquid properties on the gas phase dispersion has been investigated in bubble column reactors. Data were obtained in two 3.0 m tall bubble columns (of diameters 0.15 m and 0.25 m) and by varying superficial phase velocities. A novel experimental technique, a quadrupole mass spectrometer, was used to measure the tracer gas concentration. Data analysis was accomplished via a simple axial dispersion model with the inclusion of a mass transfer term. Results indicate that an increase in liquid viscosity and decrease in the liquid surface tension leads to a decrease in the gas phase dispersion. Further, the gas properties have no influence on the gas phase dispersion so long as the mass transfer effects are properly accounted for in the model.

A hydrodynamic model has been proposed to predict the gas phase dispersion in bubble column reactors. The model distinguishes various bubble fractions present in the column based on the differences in their rise velocities. The model assumes a bimodal distribution of the gas phase, i.e. fast-rising bubbles following a plug-flow behavior and slow-rising bubbles which are being entrained and partially backmixed in the liquid phase. The model has been validated by predicting experimental as well as literature data on gas phase dispersion under various operating conditions. The proposed model is easy to use since it requires few easily obtainable parameters for the prediction of gas phase dispersion, which is an essential parameter in the design and upscaling of bubble column reactors.

*Keywords:* Bubble column; Gas-phase dispersion; Phase property effect; Two bubble classes; Hydrodynamic modeling

## 1. Introduction

The popularity of bubble column reactors as industrial scale absorbers, fermenters, strippers, scrubbers and gas–liquid reactors is considerably growing as various aspects of these reactors are being investigated. Most of these studies are, however, limited to air–water systems, despite the fact that most bubble columns in industry are operated under a wide range of fluid properties. One of the important parameters for a proper design of bubble column reactors is the extent of backmixing in individual phases. The liquid phase mixing has been studied extensively; however, a limited amount of information exists in the literature regarding the gas phase dispersion. Moreover, the effect of individual phase properties on gas dispersion has not been addressed in the literature.

A recent paper [1] has introduced novel experimental and analytical techniques for interpreting gas phase dispersion data. It accounts for the solubility of the tracer gas, and the dispersion has been predicted using a hydrodynamic theory. Only air–water dispersion data were collected and analyzed in the previous investigation. This study extends the method to two other liquids: non-coalescing aqueous alcohol solutions, and viscous, non-newtonian carboxymethyl cellulose (CMC) solutions. The study also uses two additional tracer gases, $CO_2$ and argon.

## 2. Literature review

The published information and data on liquid phase backmixing in bubble columns together with numerous empirical correlations and hydrodynamic models are abundantly available in literature. Unfortunately, very little has been studied about the gas phase dispersion. The existing literature data on gas phase dispersion in bubble columns are scarce, mainly because of the difficulty in measuring the extent of gas phase back-

* Corresponding author.


*SSDI* 0923-0467(94)02922-9

mixing. Most of the work on gas phase backmixing has been conducted in the air–water system. Experimental measurements of the gas phase backmixing have been conducted in bubble columns ranging in diameter from 0.05 to 3.2 m. The superficial gas velocity has been varied between 0.01 and 0.13 m $s^{-1}$. Recently, Shetty et al. [1] have documented an extensive review of the previous work regarding gas phase dispersion in bubble columns. Therefore, in this section, the systems other than air–water have been discussed with their relative merits.

The gas phase dispersion is caused by (a) liquid circulation patterns and (b) coalescence and breakage of bubbles [2]. Variation in system physical properties alters the gas hold-up structure, which directly influences the gas phase backmixing. Indirectly, the physical properties are responsible for the bubble breakage–coalescence phenomena, which affect the extent of mixing in the gas phase. The surface-active agents (such as alcohols) accumulate at the gas–liquid interface and form very rigid, immobile bubble boundaries and suppress the coalescence. On the contrary, viscous non-newtonian fluids (such as CMC) promote coalescence of small bubbles to form large bubbles. These changes in bubble sizes and their rise velocities strongly influence the existing hydrodynamics in bubble columns.

Towell and Ackerman [3] have qualitatively discussed the effects of physical properties of individual phases on the gas phase dispersion. In bubble columns, the buoyancy force is mainly determined by the liquid density, and, hence, the changes in gas properties would have little or no effect on gas dispersion. The only gas phase pertinent variables are the gas flow rate and its solubility in the liquid phase. Vermeer and Krishna [4] have experimentally measured the gas phase residence time distribution (RTD) curves in the nitrogen–turpentine 5 system using a tracer gas technique. They used several tracer gases to observe the effect of gas solubility on the RTD curve. A visual inspection of the reported RTD curves indicated that, with increasing gas solubility, the RTD peak shape decreases in size and appears to be less distinct, and, at the same time, a second plateau-like distribution starts to develop and broadens the RTD tail portion. The effect of gas solubility on the gas phase dispersion was, however, not investigated using these RTD curves.

Mangartz and Pilhofer [5] have measured the gas phase dispersion in air–water, nitrogen–*n*-propanol, and air–glycol (newtonian) systems. They observed almost a three- to tenfold increase in the gas phase dispersion value for alcohol and viscous systems under churn–turbulent regimes. Also, the gas hold-up showed a decreasing trend with an increase in liquid viscosity and decrease in liquid surface tension. Recently, Mikio and Tsutao [6] have investigated the gas phase RTD in 0.16 m and 0.29 m diameter bubble columns using Fourier transforms. In addition to tap water, aqueous solutions of sodium sulfate and CMC were also used as the liquid phase. The gas hold-up in air–CMC system was reported to be lower than that for air–water. They employed an optimization procedure to predict the dispersion coefficients of small and large bubbles. Based on rather limited data, they did not reach any conclusions as to the effect of liquid properties on gas phase dispersion.

Although great progress has been made in studying the effect of liquid properties on gas hold-up and mass transfer characteristics in bubble columns, the literature still lacks an understanding of the gas phase dispersion in systems of various properties. In the present study, gas phase experimental data for viscous non-newtonian and alcohol systems are provided. Both hydrodynamic (i.e. gas hold-up and bubble rise velocities) and gas phase dispersion characteristics have been investigated together with the development of a hydrodynamic model for the prediction of gas phase dispersion in bubble columns.

## 3. Experimental set-up

All measurements were performed in two cylindrical, open-ended columns of 0.15 m and 0.25 m inner diameter, with cocurrent upflow of both phases. The superficial gas velocity ranged from 0.01 to 0.18 m $s^{-1}$. Tap water, aqueous alcohol and CMC solutions of lower concentrations were used as the liquid phase. The superficial liquid velocity was varied from 0.005 to 0.03 m $s^{-1}$. A schematic diagram of the experimental set-up is shown in Fig. 1. Measurement of the gas phase backmixing was carried out by detecting tracer gas concentration in the quadrupole mass spectrometer. Helium, argon and carbon dioxide were used as the tracer gases. The relevant properties of the tracer gases are reported by Joseph and Shah [7]. Collection of experimental data, i.e. the tracer gas RTD and the determination of phase hold-ups, has been described in detail elsewhere [1].

Very low concentrations of aqueous alcohol in water were used and hence the properties were not different from those of tap water except for low values of surface tension as shown in Table 1. The aqueous CMC solutions were prepared by slowly dissolving required quantities of the polymer powder in tap water. It should be noted that the rheological properties of CMC solutions are very sensitive to the molecular weight and the mode of preparation used, and the actual measured values are considered to be more accurate than those reported in the literature. The rheological properties of CMC solutions were measured using a concentric cylinder viscometer. The liquid density was measured using a hydrometer, and the surface tension was measured

Table 1
Relevant properties of liquid phase

| Liquid phase used and concentration (wt.%) | Flow behavior index $n$ | Consistency index $K$ (Pa $s^n$) | Density (kg $m^{-3}$) | Surface tension (N $m^{-1}$) | Viscosity (Cp) |
|---|---|---|---|---|---|
| CMC | | | | | |
| 0.05 | 0.8354 | 0.0083 | 1000 | 0.0664 | As per Eq. (3) |
| 0.10 | 0.7486 | 0.0306 | 998.5 | 0.0692 | As per Eq. (3) |
| 0.20 | 0.6679 | 0.1059 | 999 | 0.0611 | As per Eq. (3) |
| 0.30 | 0.6955 | 0.1573 | 999 | 0.0571 | As per Eq. (3) |
| 0.50 | 0.7005 | 0.1551 | 1000 | 0.0693 | As per Eq. (3) |
| Alcohols | | | | | |
| Ethanol | | | | | |
| 0.2 | – | – | 993.7 | 0.0618 | 0.85 |
| *n*-butanol | | | | | |
| 0.0012–0.36 | – | – | 994 | 0.0617 | 0.85 |

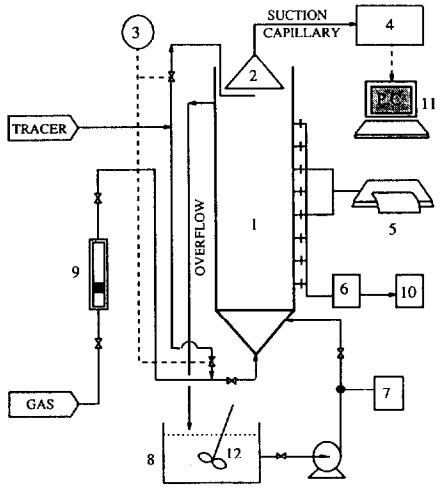


Fig. 1. Experimental set-up.

using the Cenco-DuNouy tensiometer. Table 1 summarizes the relevant properties of liquids of different concentrations used in this investigation.

The flow behavior of dilute CMC solutions was characterized by the power law model of Ostwald–de Waele as

$$\tau_s = K\dot{\gamma}^n \quad \text{and} \quad \mu_{APP} = K\dot{\gamma}^{n-1} \tag{1}$$

The apparent viscosity $\mu_{APP}$ of CMC solution was calculated using Nishikawa et al.'s [8] relation, where the average shear rate in the bubble column was related to gas velocity as

$$\dot{\gamma} = 5000U_G \tag{2}$$

Therefore, from Eqs. (1) and (2)

$$\mu_{APP} = K(5000U_G)^{n-1} \tag{3}$$

Depending on the gas velocity and the CMC concentration, the apparent viscosity varied between 0.003 Pa s and 0.04 Pa s.

## 4. Data analysis

The gas phase RTD data have been analyzed using a simple, one-dimensional, two-parameter axial dispersion model which includes the tracer gas solubility in the liquid phase. The two parameters included in the model were the gas phase axial dispersion coefficient as the Péclet number Pe, and the volumetric mass transfer coefficient as the Stanton number St. The mass balance equations in a dimensionless form are as follows: for the gas phase,

$$\frac{1}{\mathrm{Pe}_G}\frac{\partial^2 y}{\partial z^2} - \frac{\partial y}{\partial z} - \frac{\mathrm{St}}{m}(y - mc) = \frac{\partial y}{\partial \theta} \tag{4}$$

and for the liquid phase,

$$\frac{U_r \epsilon_r}{\mathrm{Pe}_L}\frac{\partial^2 c}{\partial z^2} - U_r \epsilon_r \frac{\partial c}{\partial z} + \frac{\mathrm{St}\,\epsilon_r}{m}(y - mc) = \frac{\partial c}{\partial \theta} \tag{5}$$

with the initial condition that at

$$\theta = 0, \quad 0 < z < 1, \quad y = 0, \quad c = 0 \tag{6}$$

and boundary conditions

$$z = 0, \quad \theta > 0$$

for the gas phase

$$y - \frac{1}{\mathrm{Pe}_G}\frac{\partial y}{\partial z} = \begin{cases} \delta(\theta) & \text{(for a pulse input)} \\ 1 & \text{(for a step input)} \end{cases} \tag{7a}$$

and

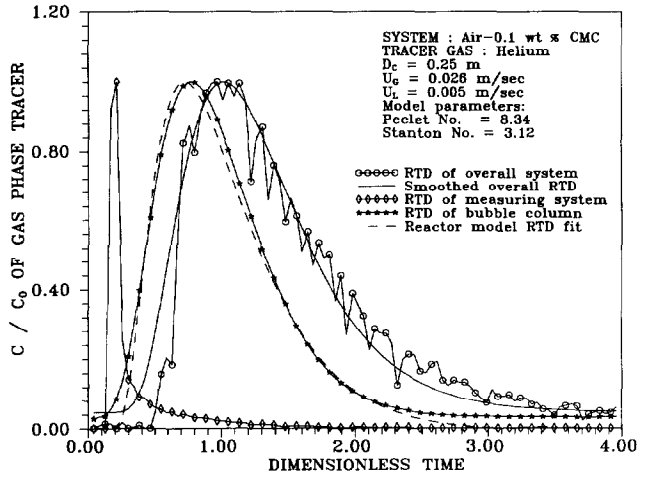


Fig. 2. Typical RTD profiles for air–CMC solution.

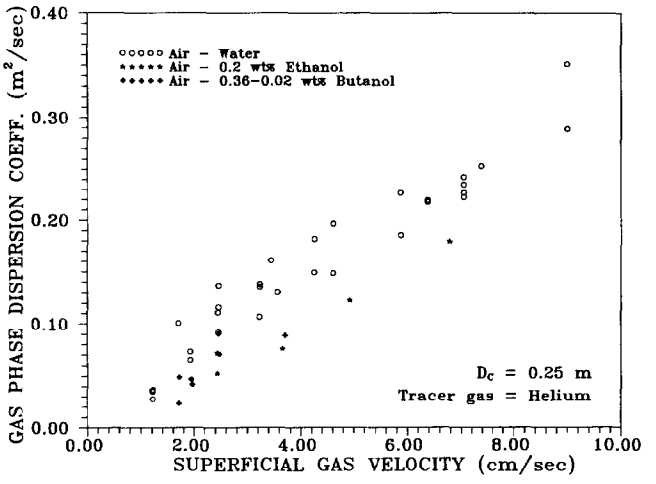


Fig. 3. Effect of the presence of alcohols on gas phase dispersion.

$$c - \frac{1}{\mathrm{Pe_L}}\frac{\partial c}{\partial z} = 0 \tag{7b}$$

for the liquid phase. Also, at $z=1$, $\theta>0$,

$$\frac{\partial y}{\partial z} = \frac{\partial c}{\partial z} = 0 \tag{7c}$$

In the above equations the dimensionless quantities defined are

$$y = \frac{UC_G}{UC_f} \quad c = \frac{UC_L}{UC_f} \quad z = \frac{x}{L} \quad \theta = \frac{U_G t}{L\epsilon_G}$$

$$\mathrm{Pe}_i = \frac{LU_i}{D_i\epsilon_i} \quad \mathrm{St} = \frac{LK_La}{U_G} \quad U_r = \frac{U_L}{U_G} \quad \epsilon_r = \frac{\epsilon_G}{\epsilon_L}$$

A detailed description of the data analysis has been reported previously [1,9] and hence is not repeated here. In summary, the noise in the raw experimental data was eliminated by a curve-smoothing technique. This was followed by a numerical deconvolution procedure which corrects for the measurement system effects, and the parameters Pe and St of the model (described by the above equations) were obtained by the Levenberg–Marquardt non-linear optimization scheme. The gas phase dispersion coefficient $D_G$ was then back calculated using the definition of Pe. A typical result for air–0.1 wt.% CMC solution is shown in Fig. 2. Similar results were obtained for other concentrations of CMC and alcohol solutions.

## 5. Results and discussion

The major thrust of this work was to illustrate the effect of column diameter, individual phase properties and their superficial velocities on the gas phase axial mixing in the bubble column. In addition, some results related to measurement of gas hold-up are also presented.

### 5.1. Gas phase dispersion

#### 5.1.1. Effect of liquid properties

Fig. 3 shows the effect of the presence of alcohols on gas phase dispersion coefficients. The data for the air–alcohol system were limited by the onset of foaming at high gas flow rates. For the air–water system, a transition from homogeneous bubble flow regime to heterogeneous churn–turbulent regime has been reported to occur at 0.04 m $s^{-1}$ gas velocity. In the presence of alcohol, however, the bubble flow regime extends up to surprisingly high gas velocities (0.08–0.1 m $s^{-1}$). All experimental data for the air–alcohol system were collected in the homogeneous bubble flow regime, wherein the uniform-sized bubbles rise without hindering each other. It is suspected that the radial variation in gas hold-up is less prominent in alcohol systems compared with that in the air–water system. Therefore, lower gas phase dispersion values are observed in the alcohol system compared with those in the air–water system. Although not shown, the effect of column diameter was negligible in the uniform bubbling regime.

Fig. 4 shows the effect of liquid viscosity on the gas phase dispersion. As the liquid viscosity increases, the gas phase dispersion decreases for a given gas flow rate. As explained in more detail in the subsequent section, at high liquid viscosity, bubbles coalesce at low gas velocities and large oblate-shaped bubbles are formed. These fast-rising bubble clusters rise in the center of the column and follow a plug-flow behavior because of their high velocity. With an increase in the liquid viscosity, the fraction of these fast-rising bubbles increases even further. This results in lower gas phase dispersion as the liquid viscosity increases.

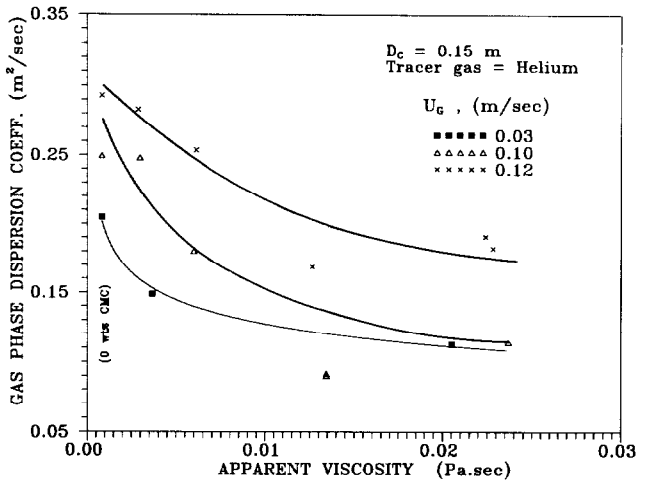


Fig. 4. Gas phase dispersion decreases with increasing liquid viscosity.

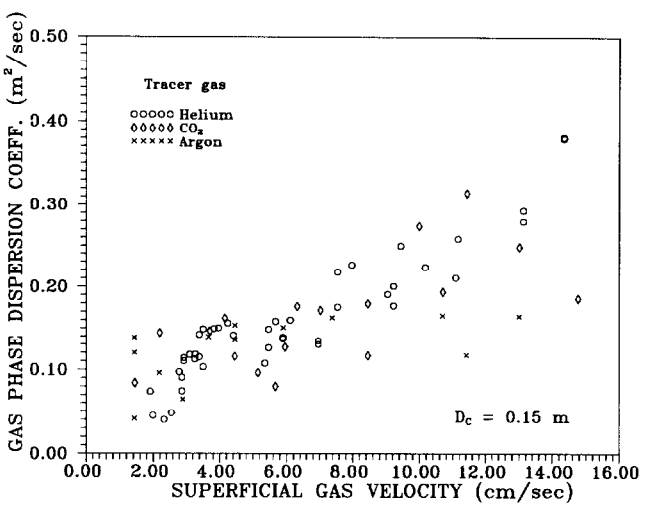


Fig. 5. Gas phase dispersion coefficients for various tracer gases.

### 5.1.2. *Effect of gas properties*

Fig. 5 demonstrates the tracer gas solubility effect on the gas phase dispersion in the air–water system. A slight variation in the dispersion values was observed while switching from almost an insoluble gas (helium) to a more soluble gas ($CO_2$). However, no significant trend was evident for both columns. This is consistent with Towell and Ackerman's observation that the gas phase should have a negligible effect on the gas phase dispersion. An increase in tracer gas solubility, however, resulted in broadening of the RTD tail portion due to enhanced mass transfer effects (Fig. 6).

Without inclusion of a mass transfer term, the effective gas phase dispersion for $CO_2$ (i.e. high solubility gas) would be calculated to be higher than that for helium. However, after properly accounting for the mass transfer term [1,7], the effect of gas properties on the gas phase dispersion was observed to be negligible. The long tailing in the $CO_2$ tracer RTD was solely due to the mass transfer effect and not because of the dispersion.

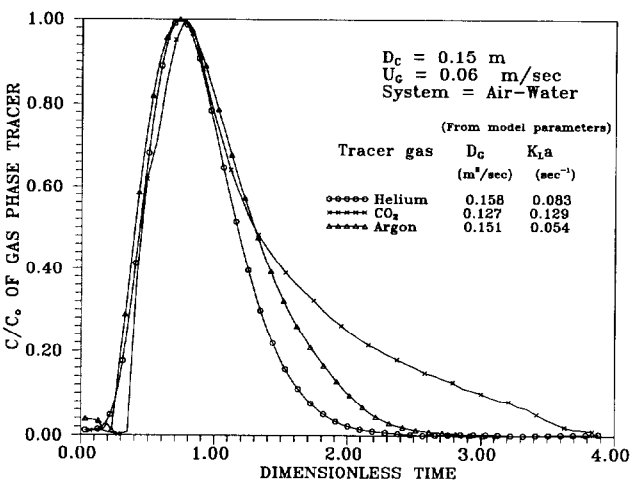


Fig. 6. Broadening effect of gas solubility on gas phase RTD.

### 5.2. *Gas hold-up*

The effect of liquid properties on the overall gas hold-up has been discussed extensively in the literature [10–14], and the results obtained during this investigation were found to be consistent with those reported previously. Thus, the results are not repeated. It suffices to state that in the presence of alcohols the gas hold-up increases, and in the presence of CMC solutions the gas hold-up decreases. In this paper, the results of the relative contributions of different bubble classes to the overall hold-up will be presented, which are used in developing the hydrodynamic model.

For the purpose of estimating the relative contributions of different bubble classes, the dynamic gas disengagement (DGD) technique of Sriram and Mann [15] was used. The DGD method is based on the assumption that the gas–liquid dispersion is axially homogeneous and there are no bubble–bubble interactions. The experimental procedure for identifying individual bubble classes is presented in detail elsewhere [1]. In this procedure, the measurement of a pressure drop across a small section of the column is made as a function of time after the gas flow has been shut off. Depending on the inflection points, the rise velocities and relative fractions of the gas hold-up for each of the bubble classes are calculated. In this analysis, two bubble classes were assumed, which are discussed later in Section 6.

Fig. 7 shows typical pressure drop profiles obtained in the DGD technique and for three systems: air–water, air–CMC and air–alcohol solutions. The profiles show two distinct rising portions corresponding to the individual bubble classes. The relative shapes and slopes of these rising patterns were found to be characteristic of the liquid properties of the system. For example, in the case of air–water system (profile A), the initial fluctuating part of the rise represents fast-rising bubble

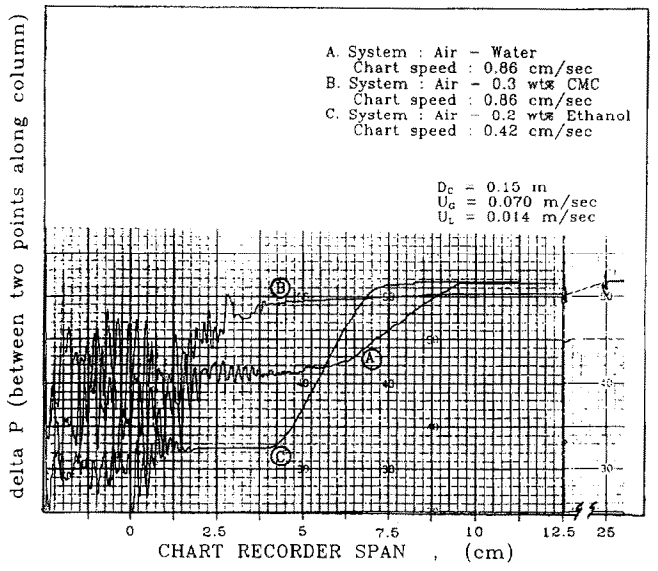


Fig. 7. Differential pressure–time traces recorded for various systems.

clusters and a smooth rising portion corresponds to the slow-rising and entrained bubble fraction. In contrast, for non-coalescing systems, such as air–alcohol (profile C), most of the rise is very smooth and gradual with initial fluctuations for a very short period of time. This implies that, for alcohol systems, the gas hold-up consists of a majority of slow-rising bubbles associated with a small contribution of fast-rising bubbles.

Viscous, non-newtonian systems, on the contrary showed entirely different DGD phenomena (profile B). It was experimentally observed during this study that, for aqueous CMC solutions up to 0.1 wt.%, the rising profiles were similar in nature to those obtained in air–water systems. However, above the CMC concentration of 0.1 wt.% in water, recorded DGD profiles indicate an initial fluctuating rise followed by a slow and asymptotic rising portion until the disengagement process is complete. This indicates that, for viscous systems, the major contribution to the overall gas hold-up comes from fast-rising bubbles, and a small fraction of the gas phase remains entrained in the viscous liquid phase for a very long time and rises slowly.

The individual contributions and rise velocities of the bubble classes were thus experimentally estimated from the DGD pressure drop profiles and are shown in Figs. 8 and 9 for air–CMC solutions. As discussed previously, the contribution of the slow-rising portion of the gas phase is small compared with the fast-rising portion. Moreover, the hold-up of slow-rising bubbles shows no increase with an increase in the gas velocity. The fast-rising bubble hold-up, however, significantly increases with increasing gas throughput. This is an indication of the enhancement of bubble coalescence with high gas throughput. Further, the rise velocity of the fast-rising portion is almost one order of magnitude

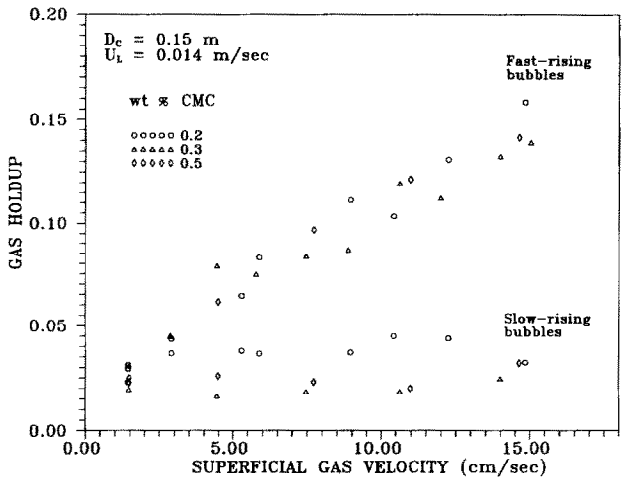


Fig. 8. Contribution of individual bubble classes to overall gas hold-up.

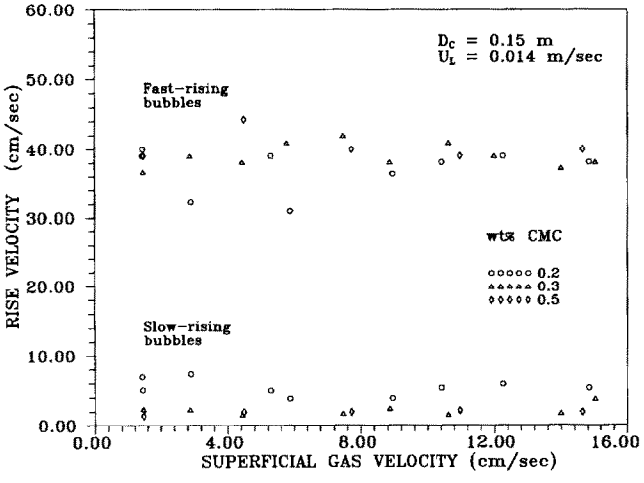


Fig. 9. Individual bubble class rise velocities for viscous system.

higher than that of slow-rising, entrained portion of the gas hold-up. Surprisingly, the relative hold-ups and rise velocities of these individual bubble fractions are not influenced by the liquid viscosity over the range studied.

## 6. Hydrodynamic model

A two-bubble-class hydrodynamic model has been proposed to predict gas phase dispersion for coalescing and non-coalescing systems in bubble columns. The major difference between the previously published theoretical model [1] and that presented here lies in the criterion used for the distinction of two bubble classes, which forms the basis of this model. Shetty et al. [1] assumed that the overall gas hold-up was contributed by two bubble classes, namely large- and small-sized bubbles. Large bubbles were assumed to rise in a plug-

flow manner, while small bubbles were partially backmixed because of the turbulence in liquid phase. Although this was the most general approach adopted by earlier researchers [4,16–18], the distinction based on the bubble sizes was artificial and unable to differentiate between the small bubbles entrained in the wake of the large bubbles and a remaining small bubble fraction that stays behind and rises slowly.

Thus, it was appropriate to distinguish two bubble classes on the basis of their rise velocities, namely fast- and slow-rising bubbles. The fast-rising bubble class, mainly, consists of highly buoyant large bubbles together with a portion of small-sized bubbles, which are trapped and accelerated in the wake of the large bubbles. The slow-rising bubble class, on the contrary, is essentially composed of the remaining fraction of the gas hold-up, which is entrained in circulating patterns of the continuous phase. It is the fast-rising fraction of the gas hold-up which causes a major gas phase transport, whereas the slow-rising fraction is, mainly, responsible for the gas entrainment in gas–liquid operations. The results of this study indicate that the distinction based on the rise velocity gives a more realistic description of the hydrodynamic behavior compared with that based on arbitrary bubble sizes.

The development and the mathematical formulation of the present hydrodynamic theory are similar to that proposed before [1] and only the modifications are discussed together with the results. The model requires a small number of input parameters to generate the gas phase RTD in bubble column reactors. Further, the use of the model does not need any experimental RTD data for the prediction of an axial gas phase dispersion. A schematic representation of the transport processes between individual bubble classes and the liquid phase is presented in Fig. 10. The following assumptions have been made in developing the model.

(1) Fast-rising bubbles follow a plug-flow behavior in the column.

(2) Slow-rising bubbles are entrained in liquid circulation patterns and are partially backmixed with an intensity equivalent to that of the liquid phase dispersion coefficient.

(3) The gas flow rate variation due to a pressure drop along the column axis is negligible.

(4) The gas hold-up remains axially homogeneous and there is no interaction between the two bubble classes.

Since the two bubble classes behave differently, each class has unique RTD characteristics, i.e. $E_1(t)$ for slow-rising bubbles and $E_2(t)$ for fast-rising bubbles. Thus, the overall gas phase RTD $E(t)$ can be described as a combination of these two RTDs based on their rise velocities and the corresponding contributions to the overall gas hold-up. Therefore

$$E(t)=(1-\alpha)E_1(t)+\alpha E_2(t) \tag{8}$$

where

$$\alpha=\frac{U_{G_2}}{U_G} \tag{9}$$

The mass balance for slow-rising bubbles is

$$\epsilon_{G_1}D_{G_1}\frac{\partial^2 C_{G_1}}{\partial x^2}-U_{G_1}\frac{\partial C_{G_1}}{\partial x}-R_1=\epsilon_{G_1}\frac{\partial C_{G_1}}{\partial t} \tag{10}$$

where

$$R_1=(K_La)_1(C^*_{L_1}-C_L) \tag{11}$$

and for fast-rising bubbles is

$$\epsilon_{G_2}D_{G_2}\frac{\partial^2 C_{G_2}}{\partial x^2}-U_{G_2}\frac{\partial C_{G_2}}{\partial x}-R_2=\epsilon_{G_2}\frac{\partial C_{G_2}}{\partial t} \tag{12}$$

where

$$R_2=(K_La)_2(C^*_{L_2}-C_L) \tag{13}$$

In Eqs. (10) and (12), the terms $R_1$ and $R_2$ are the mass flow terms accounting for the mass transfer between individual bubble classes and the liquid phase.

The mass balance equation for the liquid phase in contact with both the bubble classes can be written as

$$\epsilon_L D_L\frac{\partial^2 C_L}{\partial x^2}-U_L\frac{\partial C_L}{\partial x}+R=\epsilon_L\frac{\partial C_L}{\partial t} \tag{14}$$

where

$$R=R_1+R_2 \text{ and } \epsilon_{G_1}+\epsilon_{G_2}+\epsilon_L=1$$

Substituting Eqs. (11) and (13) in Eqs. (10), (12) and (14), and appropriately defining dimensionless quantities, the dimensionless mass balance equations take the following form: for the slow-rising bubble class

$$\frac{1}{\mathrm{Pe}^*_{G_1}}\frac{\partial^2 y_1}{\partial z^2}-\frac{\phi_1}{\gamma_1}\frac{\partial y_1}{\partial z}-\frac{\mathrm{St}_1^*}{m\gamma_1}(y_1-mc)=\frac{\partial y_1}{\partial \theta} \tag{15}$$

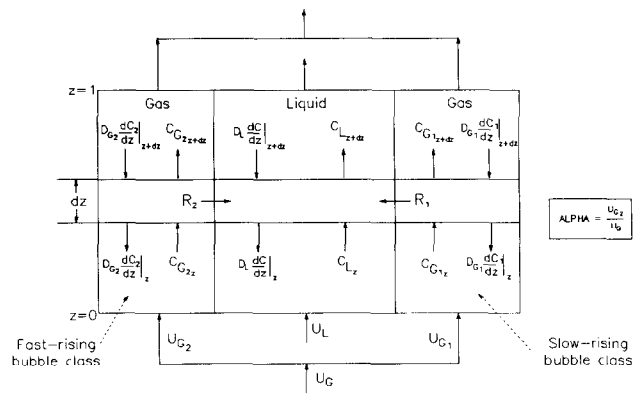


Fig. 10. Transport processes for two-bubble-class model.

for the fast-rising bubble class

$$\frac{1}{Pe^*_{G_2}}\frac{\partial^2 y_2}{\partial z^2} - \frac{\phi_2}{\gamma_2}\frac{\partial y_2}{\partial z} - \frac{St_2^*}{m\gamma_2}(y_2 - mc) = \frac{\partial y_2}{\partial \theta} \quad (16)$$

Fast-rising bubbles are assumed to be in plug-flow, in which case the gas phase mass balance Eq. (16) reduces to

$$-\frac{\phi_2}{\gamma_2}\frac{\partial y_2}{\partial z} - \frac{St_2^*}{m\gamma_2}(y_2 - mc) = \frac{\partial y_2}{\partial \theta} \quad (17)$$

For the liquid phase

$$\frac{U_r \epsilon_r}{Pe_L}\frac{\partial^2 c}{\partial z^2} - U_r \epsilon_r \frac{\partial c}{\partial z} + \frac{St_1^* \epsilon_r}{m}(y_1 - mc) + \frac{St_2^* \epsilon_r}{m}(y_2 - mc) = \frac{\partial c}{\partial \theta} \quad (18)$$

with the initial condition that at

$\theta = 0, \quad 0 < z < 1, \quad y_1 = 0, \quad y_2 = 0$ and $c = 0$

and boundary conditions as follows.

(a) $z = 0, \ \theta > 0$

For a pulse input, the gas phase balance is

$$y_1 - \frac{1}{Pe^*_{G_1}}\frac{\partial y_1}{\partial z} = \delta(\theta), \quad y_2 = \delta(\theta)$$

and the liquid phase balance is

$$c - \frac{1}{Pe_L}\frac{\partial c}{\partial z} = 0$$

(b) $z = 1, \quad \theta > 0, \quad \frac{\partial y_1}{\partial z} = \frac{\partial y_2}{\partial z} = 0,$ and $\frac{\partial c}{\partial z} = 0$

In the above equations most of the dimensionless quantities are defined previously following Eq. (4), except for two which are defined as follows:

$$\phi_i = \frac{U_{G_i}}{U_G}, \quad \gamma_i = \frac{\epsilon_{G_i}}{\epsilon_G}$$

In reality, the liquid phase is partially backmixed. An assumption of perfect liquid mixing, however, reduces the complexity involved in solving the model equations without any significant changes in model predictions [7]. Thus, an assumption of a complete liquid phase backmixing simplifies Eq. (18) as

$$-U_r \epsilon_r c + \frac{St_1^* \epsilon_r}{m}\int_0^1 (y_1 - mc)\, dz + \frac{St_2^* \epsilon_r}{m}\int_0^1 (y_2 - mc)\, dz = \frac{dc}{d\theta} \quad (19)$$

The residence time distributions of two bubble classes were generated by solving Eqs. (15), (17) and (19) in the Laplace domain. The analytical solutions were numerically inverted into the time domain using the Stehfest algorithm [19].

The model parameters include dispersion coefficient of slow-rising bubbles (assumed to be equal to the liquid phase backmixing), the individual bubble class hold-ups and volumetric mass transfer coefficients, and the fast-rising bubble contribution $\alpha$ to the overall gas throughput. The correlation proposed by Kantak et al. [20], which covered a wide range of literature data, has been used to determine the dispersion coefficient of the slow-rising bubble fraction:

$$D_{G_1} = D_L = 0.2 D_C^{1.25}\frac{U_G}{\epsilon_G} \quad (20)$$

The individual bubble class hold-ups and their rise velocities were experimentally determined from the DGD technique, and the value of $\alpha$ was evaluated using Eq. (9). The nature of the predicted RTD strongly depends on the value of $\alpha$. $\alpha = 0$ implies that only slow-rising bubbles exist, i.e. the flow is in the homogeneous regime. In contrast, $\alpha = 1$ implies that the entire gas phase follows a plug-flow behavior in the form of fast-rising bubbles. Previously reported values of the volumetric mass transfer coefficients [1] have been used in this work. The predicted profiles were later found to be insensitive to the individual bubble class volumetric mass transfer coefficients.

The proposed model was applied for the prediction of RTD data reported by Mikio and Tsutao [6] in a viscous system. The experimental data for a 0.16 m diameter column and 0.03 m $s^{-1}$ gas velocity were digitized and used for the analysis. The gas phase RTD was generated by using the proposed model for the model parameters reported in Ref. [6]. Fig. 11 shows that the two-bubble-class model reproduced these authors' RTD peak, representative of the gas phase dispersion, and also an experimentally observed "hump"

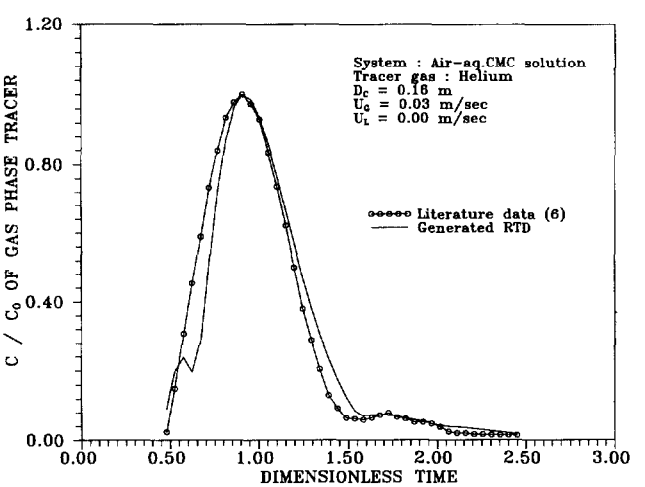


Fig. 11. Prediction of literature data [6] using proposed model.

in the later part of their RTD profile. The "hump" was thus recognized to be due to the slow-rising bubble contribution in overall gas hold-up. It was interesting to note that the previous model [1] was unable to reproduce these authors' RTD tail portion and the experimentally observed "hump".

In addition, the experimental RTD data obtained during this investigation were also analyzed using the proposed model. Fig. 12 shows a match between the experimental data for air–butanol system and the generated profile for $\alpha=0$, whereas Fig. 13 shows the comparison between the predicted and experimental profiles for air–0.5 wt.% CMC solution. A high value of $\alpha$, for 0.045 m $s^{-1}$ gas velocity, implies that an increase in the liquid viscosity causes more gas bubbles to coalesce and to form a large body of fast-rising bubbles in the column. In viscous liquids, both the shear stresses in the liquid and the formation of instabilities at the gas–liquid interface are dampened, and bubble break-up occurs less frequently. The expected increase in the fast-rising bubble contribution therefore leads to a high value of $\alpha$, which eventually approaches the unity.

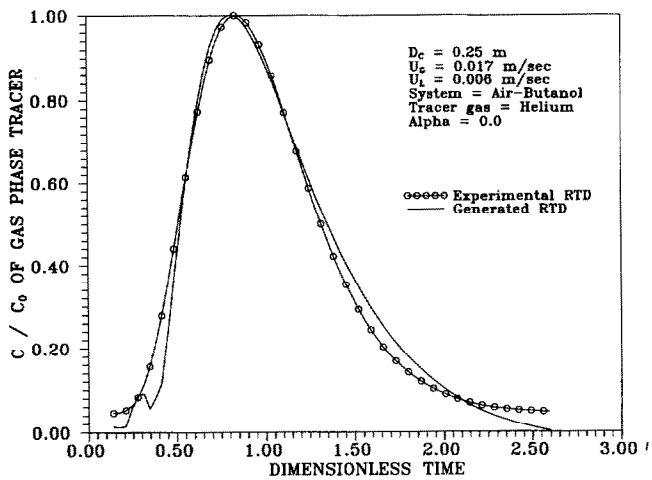


Fig. 12. Model prediction for non-coalescing system.

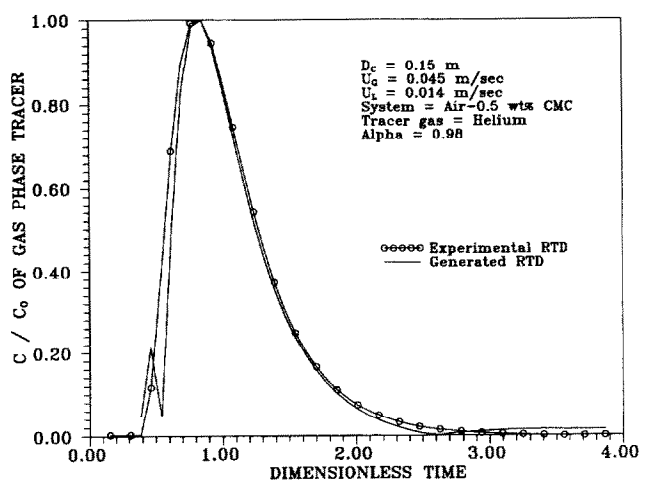


Fig. 13. Model prediction for viscous, non-newtonian system.

Although not shown, significant effects of the gas velocity and the column diameter on the value of $\alpha$ were observed in air–CMC systems. For the gas velocity of 0.085 m $s^{-1}$ and for 0.05 wt.% CMC concentration, the $\alpha$ values obtained for 0.15 m and 0.25 m diameter columns were 0.46 and 0.37 respectively. This implies that, for small columns, the bubble coalescence frequency increases as more and more bubbles come into a position favorable for coalescence. Also, the $\alpha$ value increased with an increase in the gas throughput. The liquid flow rate, however, showed no significant effect over the range studied.

Model predictions for other experimental cases have been documented elsewhere [9], and are not repeated here. In summary, the present hydrodynamic theory, using a novel and realistic approach, satisfactorily predicts the gas phase dispersion characteristics in two-phase systems. Also, a comparison of results obtained using the proposed model and that presented previously [1] shows that the present approach is much better in terms of predicting the peak and the long tail portion of the gas phase RTD profiles.

## 7. Conclusions

The results obtained in this investigation are summarized below.

### *7.1. Gas phase dispersion*

– The existence of an extended bubble flow regime is the main reason for low gas phase dispersion coefficients in air–alcohol systems.
– Increase in liquid viscosity enhances the coalescence of gas bubbles, which results in a decrease in gas phase dispersion.
– The effect of gas solubility on the gas phase dispersion is negligible.

### *7.2. Gas hold-up*

– The overall gas hold-up increases with decreasing liquid surface tension. An increase in the liquid viscosity, however, causes overall gas hold-up to decrease.

### *7.3. Bubble class contribution and rise velocity*

– The presence of alcohols suppresses bubble coalescence, which results in a high contribution of slow-rising bubbles to the overall gas hold-up.
– Increasing liquid viscosity increases the fast-rising bubble contribution in overall gas hold-up.

– Rising velocities of individual bubble classes are not influenced either with changing column diameter or liquid viscosity, but are affected by the superficial gas velocity.

### 7.4. *Hydrodynamic modeling*

In comparison with the previous model [1], the present theory developed on the principle of fast- and slow-rising bubble fractions predicts both experimental and literature data with a better accuracy than the previous model. The model is easy to implement with a small number of easily obtainable input parameters. These parameters could either be measured in small diameter columns (say, 0.1 m diameter) or could be obtained from the existing literature. Further, the proposed model could be extended for other reactor configurations so long as the required model parameters are known.

## Acknowledgements

The financial assistance provided by the National Science Foundation throughout the course of this research and facilities provided by the University of Tulsa are gratefully acknowledged. Also, authors thank the anonymous reviewer of the earlier versions of this manuscript for valuable suggestions, which resulted in a significant improvement of the proposed model.

## Appendix A: Nomenclature

| | |
|---|---|
| $a$ | gas–liquid interfacial area ($cm^2\ cm^{-3}$) |
| $c$ | normalized liquid phase tracer concentration |
| $C$ | concentration of tracer (kmol $m^{-3}$) |
| $C_f$ | reference concentration of tracer (kmol $m^{-3}$) |
| $C^*$ | equilibrium concentration at the gas–liquid interface (kmol $m^{-3}$) |
| $C_o$ | maximum concentration of tracer (kmol $m^{-3}$) |
| $D_C$ | column diameter (m) |
| $D_G$ | gas phase dispersion coefficient ($m^2\ s^{-1}$) |
| $D_L$ | liquid phase dispersion coefficient ($m^2\ s^{-1}$) |
| $E(t)$ | non-dimensional residence time distribution |
| $K_La$ | liquid side volumetric mass transfer coefficient ($s^{-1}$) |
| $L$ | gas–liquid dispersion height (m) |
| $m$ | Henry's law constant ($m^3$ liquid ($m^3$ gas)$^{-1}$) |
| $Pe_i$ | $LU_i/D_i\epsilon_i$, Péclet number |
| $Pe^*_{G_i}$ | $LU_G/D_{G_i}\epsilon_G$, modified Péclet number |
| $R$ | rate of mass transfer (kmol $m^{-3}\ s^{-1}$) |
| $St^*$ | $L(K_La)_i/U_G$, modified Stanton number |
| $t$ | time (s) |
| $U$ | superficial phase velocity ($m\ s^{-1}$) |
| $U_r$ | dimensionless velocity |
| $x$ | distance along the column length (m) |
| $y$ | dimensionless tracer gas concentration |
| $z$ | dimensionless axial column length |

*Greek symbols*

| | |
|---|---|
| $\alpha$ | $U_{G_2}/U_G$, superficial velocity ratio of fast-rising bubble fraction to overall gas |
| $\gamma$ | $\epsilon_{G_i}/\epsilon_G$, ratio of individual bubble class to overall gas hold-up |
| $\dot{\gamma}$ | shear rate ($s^{-1}$) |
| $\delta$ | Dirac delta function |
| $\epsilon$ | phase hold-up |
| $\epsilon_r$ | $\epsilon_G/\epsilon_L$, relative phase hold-up |
| $\theta$ | dimensionless time |
| $\mu_{APP}$ | apparent viscosity of non-newtonian fluids (Pa s) |
| $\tau_s$ | shear stress (Pa) |
| $\phi$ | $U_{G_i}/U_G$, superficial velocity ratio of individual bubble class to overall gas |

*Subscripts*

| | |
|---|---|
| G | gas phase |
| L | liquid phase |
| 1 | slow-rising bubble phase |
| 2 | fast-rising bubble phase |

## References

[1] S.A. Shetty, M.V. Kantak and B.G. Kelkar, *AIChE J., 38* (1992) 1013.
[2] J.B. Joshi, A.B. Pandit and K. Raghav Rao, in N.P. Cheremisinoff (ed.), *Encyclopedia of Fluid Mechanics*, Vol. 3, Gulf Publishing, 1986, p. 1137.
[3] G.D. Towell and G.H. Ackerman, *Proc. 5th Eur.–2nd Int. Symp. on Chem. Eng.*, Elsevier, Amsterdam, 1972, p. B3-1.
[4] D. Vermeer and R. Krishna, *Ind. Eng. Chem. Process Des. Dev., 20* (1981) 475.
[5] K.H. Mangartz and Th. Pilhofer, *Chem. Eng. Sci., 36* (1981) 1969.
[6] K. Mikio and O. Tsutao, *German–Japanese Symp. on Bubble Columns*, Schwerte, Germany, 1988, p. 257.
[7] S. Joseph and Y.T. Shah, *Can. J. Chem. Eng., 64* (1986) 380.
[8] M. Nishikawa, H. Kato and K. Hashimoto, *Ind. Eng. Chem. Process Des. Dev., 16* (1977) 133.
[9] M.V. Kantak, *M.S. Thesis*, University of Tulsa, 1992.
[10] B.G. Kelkar, S.P. Godbole, M.F. Honath, Y.T. Shah, N.L. Carr and W.-D. Deckwer, *AIChE J., 29* (1983) 361.
[11] B. Konig, R. Buchholz, J. Lucke and K. Schugerl, *Ger. Chem. Eng., 1* (1978) 199.
[12] S.P. Godbole, M.F. Honath and Y.T. Shah, *Chem. Eng. Commun., 16* (1982) 119.
[13] S.P. Godbole, A. Schumpe, Y.T. Shah and N.L. Carr, *AIChE J., 30* (1984) 213.
[14] B.G. Kelkar and Y.T. Shah, *AIChE J., 31* (1985) 700.
[15] K. Sriram and R. Mann, *Chem. Eng. Sci., 32* (1977) 571.
[16] J. Joseph and Y.T. Shah, *ACS Symp. Ser., 27* (1984) 149.
[17] O. Molerus and M. Kurtin, *Chem. Eng. Sci., 41* (1986) 2685.
[18] S.A. Patel, J.D. Daly and D.B. Bukur, *AIChE J., 35* (1989) 931.
[19] M. Stehfest, *Commun. ACM., 13* (1970) 47.
[20] M.V. Kantak, S.A. Shetty and B.G. Kelkar, *Chem. Eng. Commun., 127* (1994) 23.